

From CO₂ to dimethyl carbonate with dialkyldimethoxystannanes: the key role of monomeric species

Mahboubeh Poor Kalhor,^a Henry Chermette,^{*a} Stéphane Chambrey^b and Danielle Ballivet-Tkatchenko^{*b}

^a Université de Lyon, Université Lyon 1 et CNRS, Sciences Analytiques-Laboratoire de Chimie Physique Théorique, 43 bd du 11 novembre 1918, 69622 Villeurbanne cedex, France

^b Université de Bourgogne et CNRS, Institut de Chimie Moléculaire, 9, av. A. Savary, 21000 Dijon, France

Table S1 Relevant geometrical parameters for **7** and **8**

Table S2 Relevant geometrical parameters for **11**

Fig. S1 Energy profile of the reaction between CO₂ and **1**, and relevant charges (in italic).

Fig. S2 Energy profile of the reaction between CO₂ and **2**, and relevant distances (Å) and charges (italic).

Fig. S3 Changes in energy and shape of HOMOs and LUMOs of CO₂ and **2** to **9**.

Fig. S4 Energy profile for the reaction of CO₂ with **3** to **9**.

Fig. S5 Energy profile for the reaction of CO₂ with **4** to **9**.

Fig. S6 Energy profile for the reaction of CO₂ with **5** to **9**.

Fig. S7 Energy profile for the reaction of CO₂ with **6** to **9**.

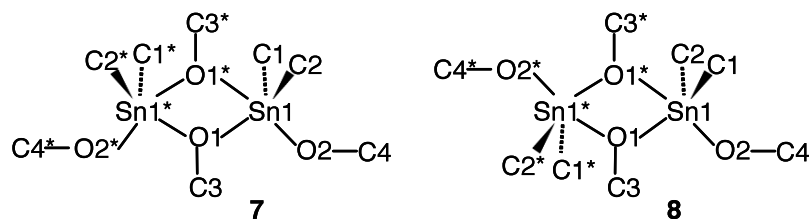
Fig. S8 Energy diagrams calculated with PW91 functional for the reaction of CO₂ with **1** to **11**.

Fig. S9 Gibbs energy diagrams for the reaction of CO₂ with **1** to **11** at 298 K.

Fig. S10 Gibbs energy diagrams for the reaction of CO₂ with **1** to **11** at 423 K.

Fig. S11 Energy profile of the reaction between CO₂ and **9**.

Table S1 Relevant geometrical parameters (Å, deg) for **7** and **8**

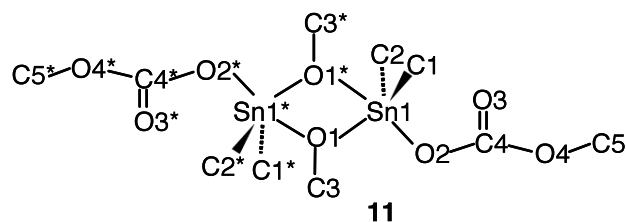


	DFT (this study)		X-Ray ^a	B3LYP ^b	MP2 ^b		DFT (this study)		X-Ray ^a
	7	8	8	8	8		7	8	8
Sn(1)-O(1)	2.146	2.089	2.038	2.034	2.027	O(1)-Sn(1)-C(2)	116.3	115.8	109.4
Sn(1)-O(1*)	2.221	2.313	2.324	2.262	2.236	O(1*)-Sn(1)-O(2)	154.9	156.3	161.7
Sn(1)-O(2)	2.067	2.064	2.038	2.002	1.999	O(1*)-Sn(1)-C(1)	90.8	89.1	86.6
Sn(1)-C(1)	2.183	2.183	2.121	2.140	2.123	O(1*)-Sn(1)-C(2)	90.8	89.1	88.3
Sn(1)-C(2)	2.183	2.183	2.13	2.140	2.126	O(2)-Sn(1)-C(1)	100.7	101.8	96.4
O(1)-C(3)	1.459	1.434	1.445			O(2)-Sn(1)-C(2)	100.7	101.8	101.8
O(2)-C(4)	1.416	1.416	1.300			C(1)-Sn(1)-C(2)	123.8	123.4	135.1
O(1)-Sn(1)-O(1*)	68.7	68.6	68.9			Sn(1)-O(1)-Sn(1*)	114.0	111.3	111.1
O(1)-Sn(1)-O(2)	86.1	87.7	93.2			Sn(1)-O(1)-C(3)	123.9	123.7	122.8
O(1)-Sn(1)-C(1)	116.3	115.8	110.0						

^a J.-C. Choi, T. Sakakura and T. Sako, *J. Am. Chem. Soc.*, 1999, **121**, 3793-3794.

^b K. Wakamatsu, A. Orita and J. Otera, *Organometallics*, 2008, **27**, 1092-1097.

Table S2 Relevant geometrical parameters (Å, deg) for **11**



	DFT	X-Ray ^a		DFT	X-Ray ^a
Sn(1)-O(1)	2.099	2.086	O(1)Sn(1)C(1)	109.6	102.1
Sn(1)-O(1*)	2.341	2.223	O(1)Sn(1)C(2)	108.2	104.6
Sn(1)-O(2)	2.173	2.192	O(1)Sn*(1)O(2*)	156.9	155.9
Sn(1)-C(1)	2.166	2.102	O(1)Sn*(1)C*(1)	89.4	91.8
Sn(1)-C(2)	2.162	2.11	O(1)Sn*(1)C*(2)	87.8	91.6
O(1)-C(3)	1.434	1.413	O(2)Sn(1)C(1)	99.8	94
O(2)-C(4)	1.306	1.292	O(2)Sn(1)C(2)	99.4	93.8
O(3)-C(4)	1.246	1.201	C(1)Sn(1)C(2)	138.2	152.8
O(4)-C(4)	1.359	1.353	Sn(1)O(1)Sn(1*)	109.6	108.2
O(4)-C(5)	1.444	1.426	Sn(1)O(1)C(3)	125.4	124.3
O(1)Sn(1)O(1*)	70	71.8	O(2)C(4)O(3)	124.7	125.9
O(1)Sn(1)O(2)	86.9	84.1	O(2)C(4)O(4)	112.4	115.9

^aJ.-C. Choi, T. Sakakura and T. Sako, *J. Am. Chem. Soc.*, 1999, **121**, 3793-3794.

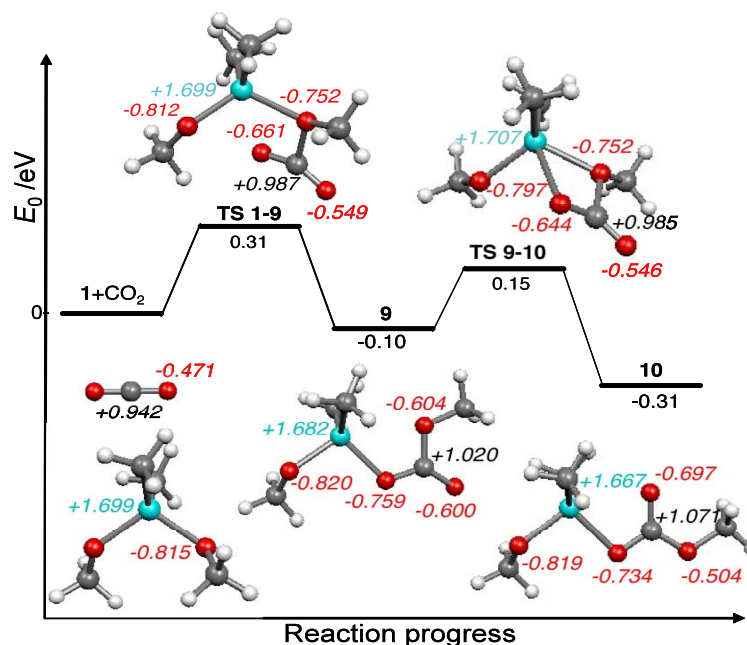


Fig. S1 Energy profile of the reaction between CO₂ and **1**, and relevant charges (in italic).

Monocarbonation of constrained structures. When **1** was constrained to adopt the geometry depicted as **2** (Figure 5), the transition state **TS 2-9** for the CO₂ insertion into one Sn-OCH₃ bond was found to be slightly more stable than **2** by 11.6 kJ mol⁻¹ (Figure S2). This result indicates that the interaction with CO₂ releases somewhat the imposed constraint. The geometry of **TS 2-9** is essentially characterized by one O atom of CO₂ approaching tin at a distance closer to the Sn-O equilibrium value (2.664 vs 2.094 Å) than that of the relevant CH₃O group (2.180 vs 1.408 Å). The interaction leads to a significant increase of the absolute charges on the atoms involved in the four-membered stannacycle of **TS 2-9**. As shown in Figure S3, the marked negative increase on the O atom of CO₂ stems from electron transfer between the HOMOs of the complex, especially HOMO-4, and the LUMO of CO₂. The electron transfer from HOMO-1 of CO₂ toward the LUMO of the complex is responsible for the increase of the negative charge on the oxygen atom of the CH₃O group. These charge transfers lead simultaneously to the increase of the positive charges on Sn and C (CO₂). Two intermediate states **IM 2-9** and **IM' 2-9** were optimised (Figure S2). Their salient feature consists in the formation of the methylcarbonate ligand in a dihapto coordination mode, the C=O bond being endocyclic. At last, comparison between the two channels **1**→**TS 1-9** and **1**→**TS 2-9** points out that the deformation of **1** to **2** prior to CO₂ insertion leads to a significant increase in the energy barrier (55 vs 30 kJ mol⁻¹). Similar findings were found for the constrained geometries **3-6** (Figures S4-S7).

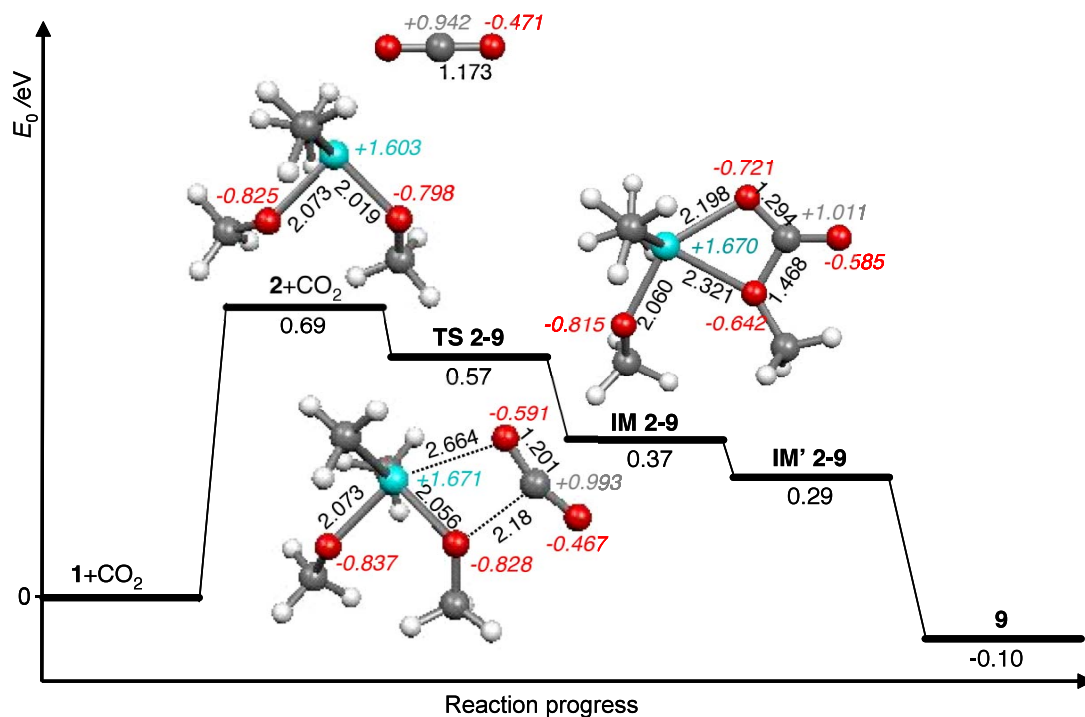


Fig. S2 Energy profile of the reaction between CO₂ and **2**, and relevant distances (Å) and charges (italic).

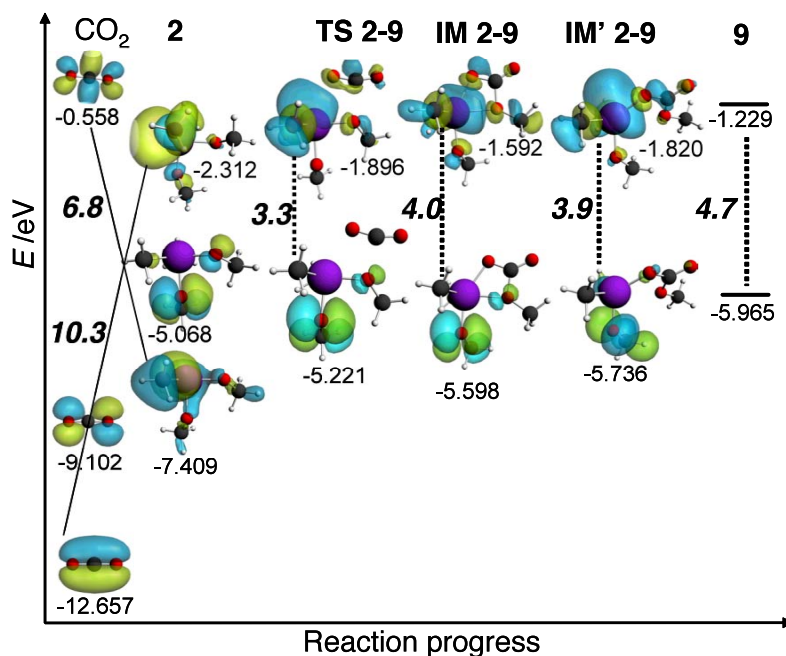


Fig. S3 Changes in energy and shape of HOMOs and LUMOs of CO₂ and **2** to **9** via TS 2-9. Are pictured: LUMO, HOMO and HOMO-1 of CO₂, LUMO, HOMO and HOMO-4 of **2**, and LUMO and HOMO of the other systems (ΔE between HOMOs and LUMOs in italic).

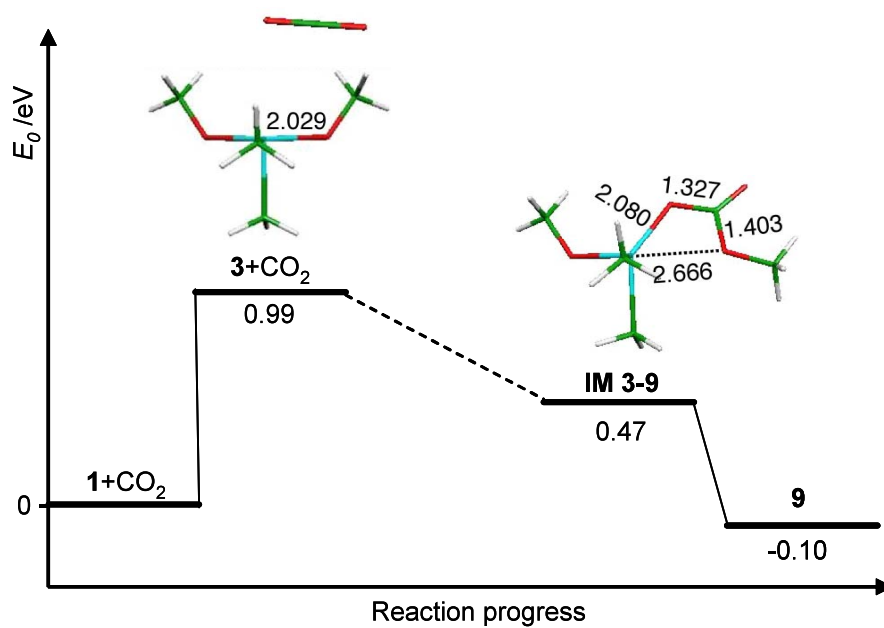


Fig. S4 Energy profile for the reaction of CO₂ with **3** to **9** (distances in Å).

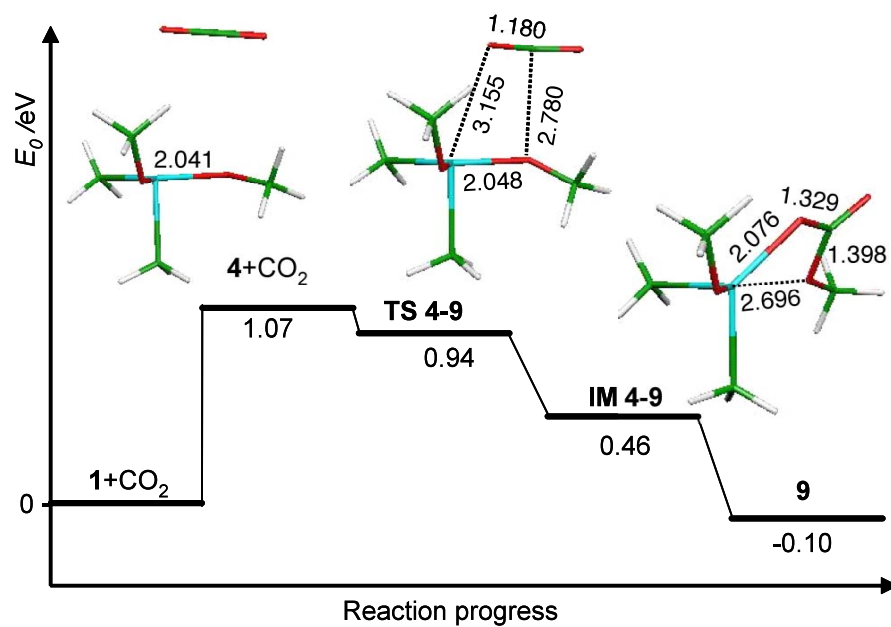


Fig. S5 Energy profile for the reaction of CO₂ with **4** to **9** (distances in Å).

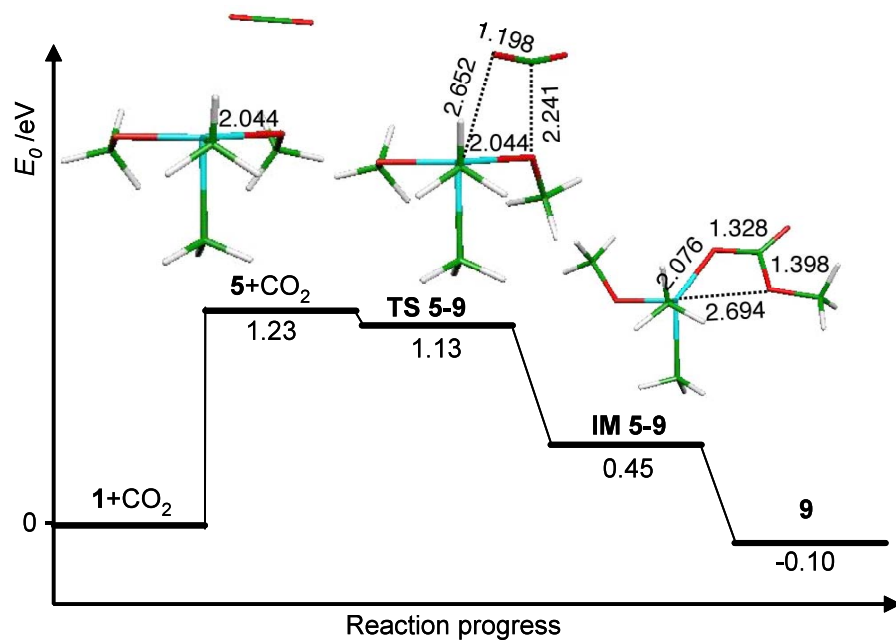


Fig. S6 Energy profile for the reaction of CO₂ with **5** to **9** (distances in Å).

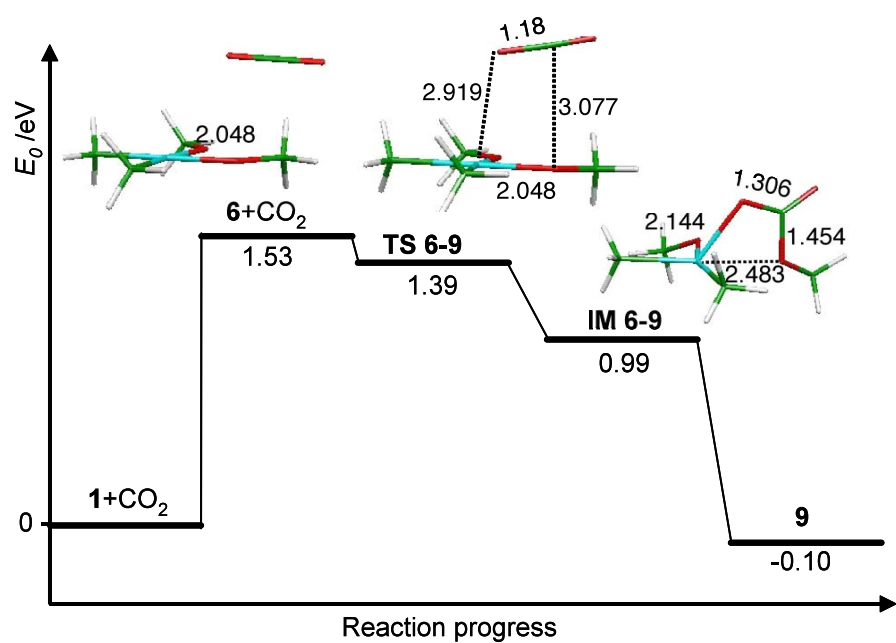


Fig. S7 Energy profile for the reaction of CO₂ with **6** to **9** (distances in Å).

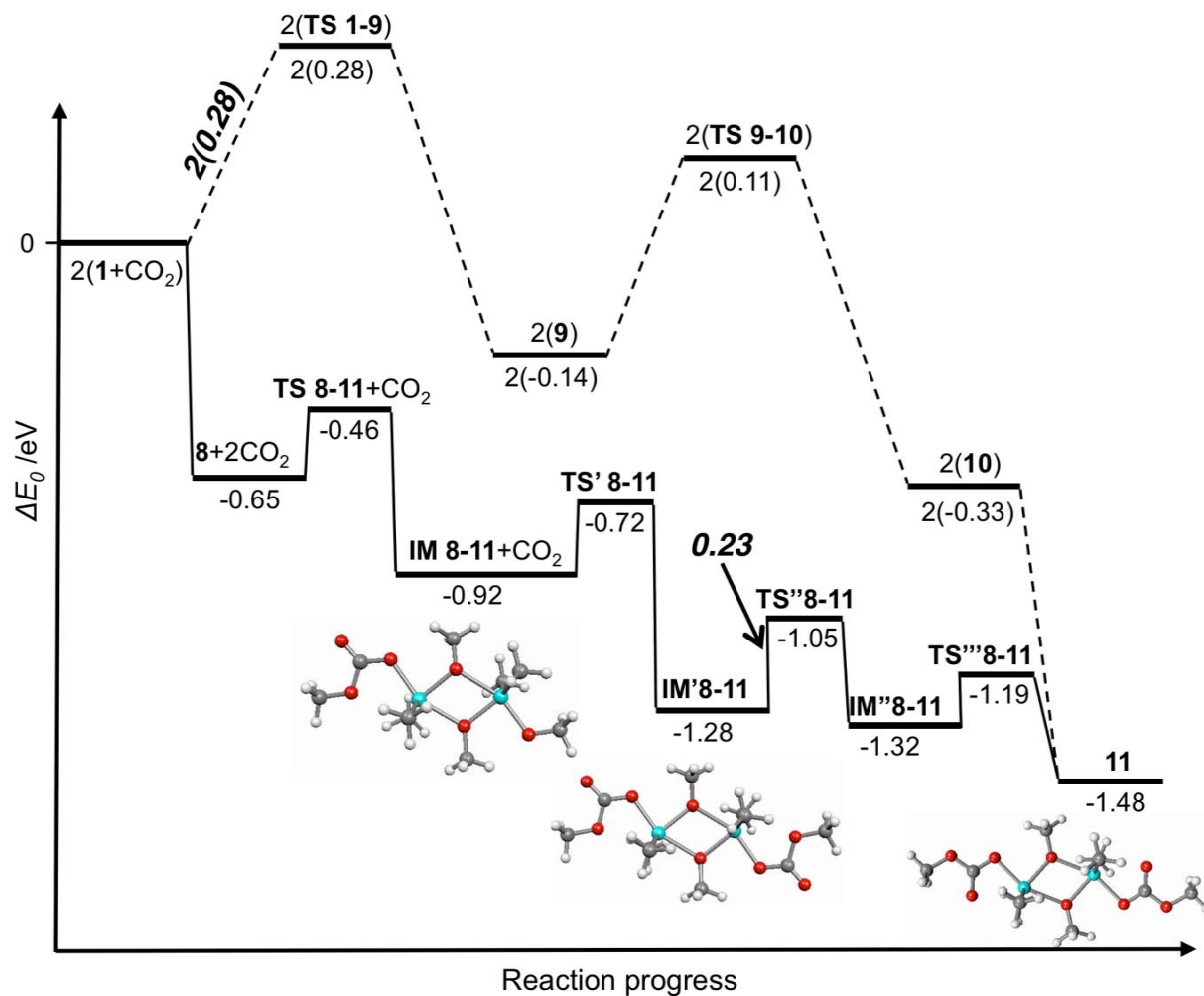


Fig. S8 The two energy diagrams calculated with PW91 functional for the reaction of CO₂ with **1** to **11**.

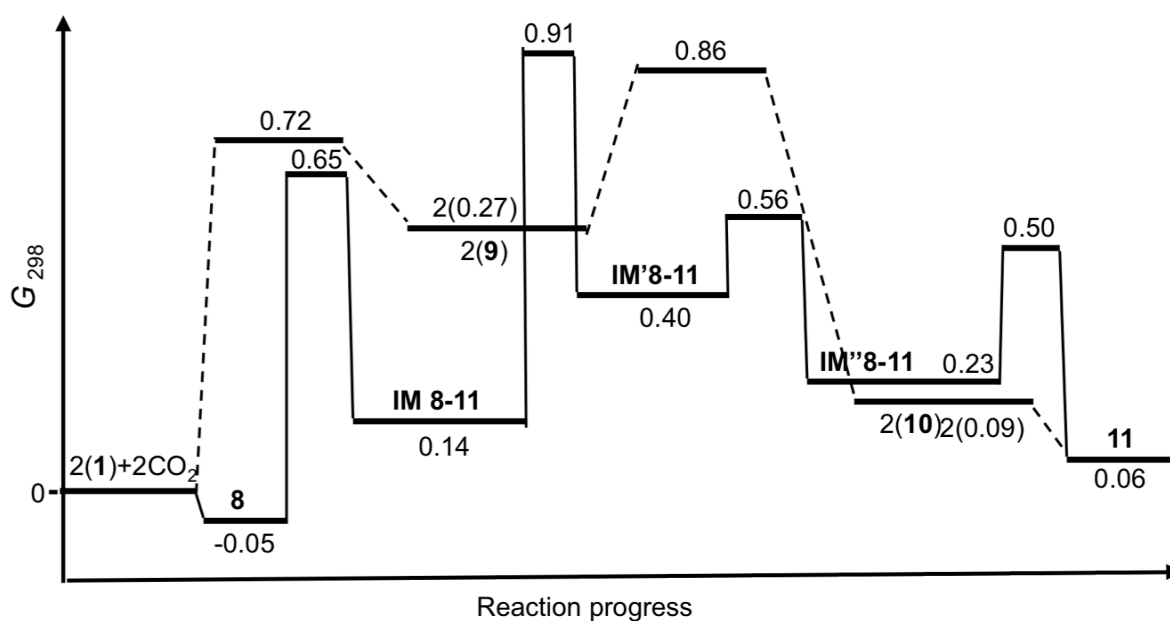


Fig. S9 The two Gibbs energy diagrams for the reaction of **1** with CO₂ to **11** at 298 K. For the route **1**→**10**→**11** the energy of states **9** and **10** is given for two complexes (for stoichiometry reason) but for the transition state the barrier is given for one complex.

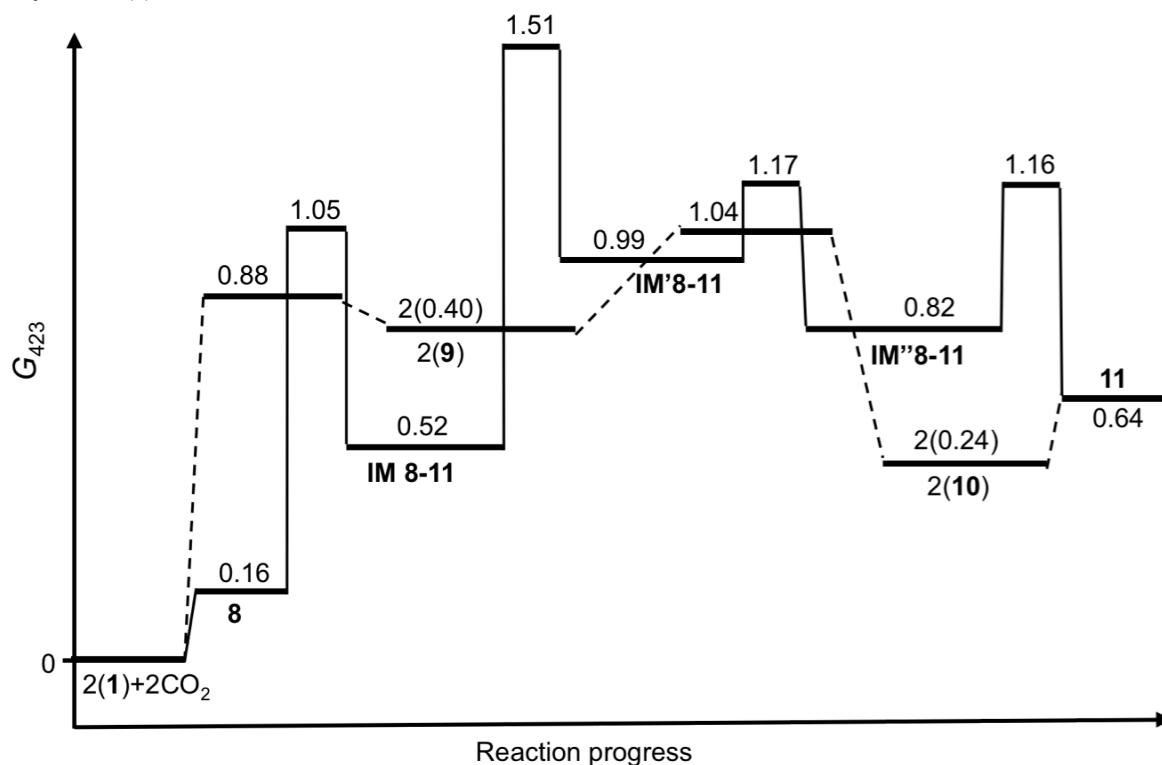


Fig. S10 The two Gibbs energy diagrams for the reaction of **1** with CO₂ to **11** at 423 K. For the route **1**→**10**→**11** the energy of states **9** and **10** is given for two complexes (for stoichiometry reason) but for the transition state the barrier is given for one complex.

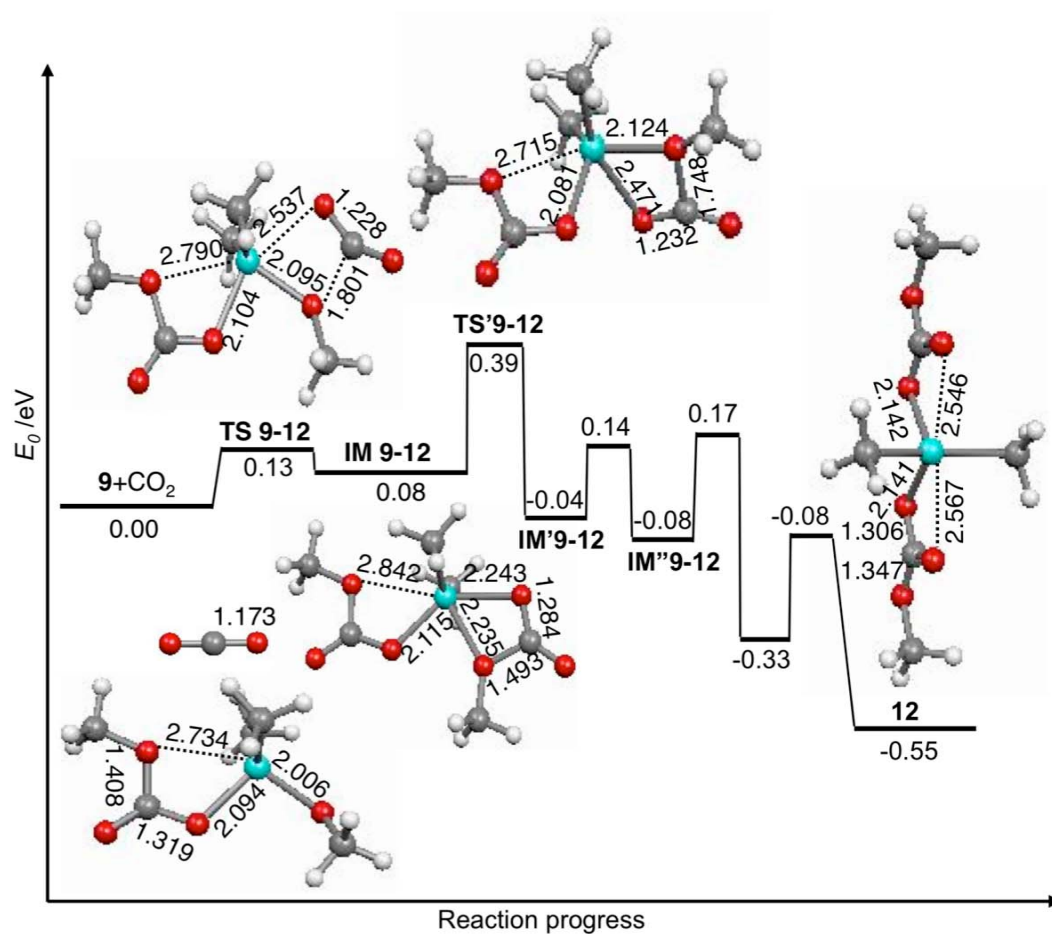


Fig. S11 Energy profile of the reaction between CO₂ and **9**, and relevant distances (Å).